Rare Decays in LHCb

U. Egede[a*]

[a]Imperial College London, London SW7 2AZ, United Kingdom

The LHCb detector has collected its first data at the collision energy of $\sqrt{s} = 7\,\text{TeV}$ and is performing very well. With a focus on the $B_s \to \mu^+\mu^-$, $B_s \to \phi\gamma$ and $B_d \to K^{*0}\mu^+\mu^-$ decays, we explain why rare decays decays are important, demonstrate the validation of the detector we have done for them, and show our expected performance with the 2010 and 2011 data.

1. Introduction

The LHCb experiment is dedicated to the exploration of heavy flavour physics, taken advantage of the very large production rate of charm and beauty hadrons in the proton-proton collisions of the LHC. The first run of the LHCis expected to last until the end of 2011 and accumulate a total integrated luminosity of $1\,\text{fb}^{-1}$.

Of particular importance is the analysis of what is broadly termed Rare Decays. By this is meant Flavour Changing Neutral Current (FCNC) decays with either photons or leptons in their final states. In the Standard Model (SM) these decays are only allowed at loop level thus setting the SM and New Physics (NP) on an equal footing. The low branching ratios but still clean signatures in the final states makes a hadron machine an ideal environment for precision physics. While LHCb will not be able to perform inclusive analysis such as the differential branching ratio of $b \to s\ell^+\ell^-$, a precision analysis can be made in exclusive modes where asymmetries can be formed to cancel out hadronic uncertainties.

A model independent analysis of rare decays, where we express the branching ratios and dynamics of the decays through the Operator Product Expansion, can be performed. In this expansion, the physics at energy scales above the B mass are expressed as an effective theory with a Lagrangian of the type

$$\mathcal{L}_{\text{eff}} = \mathcal{L}_{\text{gauge}} + \mathcal{L}_{\text{Higgs}} + \sum_{n,d>4} \frac{\mathcal{C}_n}{\Lambda^{d-4}} \mathcal{O}_n^d\,, \quad (1)$$

where Λ is the energy scale of NP, $\mathcal{O}_n^d$ all possible operators of dimension d and $\mathcal{C}_n$ the corresponding Wilson coefficients. The influence of the Z^0 and $W^\pm$ vector bosons as well as the top quark will of course mean that even in the SM, the Wilson coefficients are non-zero. The challenge of any analysis is to device it in a way, where the sensitivity to the Wilson coefficients is high, while the theoretical uncertainty from hadronic interactions is kept minimal. Rare decays are sensitive to the Wilson coefficients $\mathcal{C}_7$, $\mathcal{C}_9$ and $\mathcal{C}_{10}$, their corresponding right handed counterparts indicated with a prime, and the scalar and pseudoscalar coefficients $\mathcal{C}_S$ and $\mathcal{C}_P$.

2. The LHCb detector

The LHCb detector is a single arm spectrometer placed at one of the four collision points of the LHC. Its acceptance is from around 10 mrad to around 250 mrad in polar angle, which covers the region with the largest cross section for B production. In this forward region the B hadrons have an average flight distance of 7 mm making

*On behalf of the LHCb collaboration.

the identification of secondary vertices easier.

Closest to the interaction point is the silicon strip vertex detector. It is constructed in two halves which are retracted during injection and ramping of the beam. Once the beam is stable it moves in such that the distance from the beam to the silicon is just 7 mm in the transverse plane. The next downstream sub-detector is a silicon strip tracking station, which is followed by the first part of the RICH detector to enable separation of charged kaons and pions. Further downstream, the particles enter a large dipole magnet followed by a further three tracking stations to measure the momentum of charged particles through their bending in the magnetic field. These tracking stations are silicon strip detectors closest to the beam pipe, where the track density is the highest, and drift tubes further out. After this the particles pass a second RICH detector with a radiator optimised for higher momentum particles. The calorimeter consist of a scintillator pad detector, a preshower, a lead/scintillator Shashlik electromagnetic calorimeter and finally an Fe/scintillator hadronic calorimeter. The calorimeter provides electron and photon identification and provides the first trigger level for electromagnetic and hadronic deacys. Finally LHCb has a large muon system consisting of five tracking stations with multi wire proportional chambers with granularity depending on the distance to the beam pipe. In total the detector is 21 m long and the last muon station has a transverse dimension of $10 \times 10\,\mathrm{m}^2$.

As the interaction rate, when LHC is fully commissioned, will be around 30 MHz and the total output rate that can be accepted from the experiment is 2 kHz, there is a large demand on the trigger system. At the first trigger level, the presence of a B decay is inferred through the presence of a lepton or a hadron with large transverse energy/momentum with respect to the beam axis. This brings the rate down to 1 MHz which then allows for a read-out of the full detector. The subsequent High Level trigger is fully implemented in software. It performs the full track reconstruction to allow for the identification of secondary vertices and the identification of specific final states through either inclusive or exclusive reconstruction. The full trigger system is illustrated in Fig. 1.

3. $B_s \to \mu^+\mu^-$

The $B_s \to \mu^+\mu^-$ decay is very sensitive to the Higgs sector of any NP model. In the SM the branching ratio has the precise prediction of $(3.6 \pm 0.4) \times 10^{-9}$ [1] which is about a factor 10 below the current 95% upper confidence limit set by CDF. Thus there is still room for a large enhancement from NP in this decay.

The search for the decay is based on a method of counting in bins of three independent variables:

Invariant mass of the muon pair The power of this variable is determined by the tracking system resolution and the alignment.

Muon identification likelihood This is dominated by the muon system but also use information from the calorimeters and the RICH detectors.

Geometrical likelihood This is a likelihood formed from quantities where the vertex detector provides the main discrimination, such as impact parameters, vertexing and lifetime.

The important points for the analysis now is to validate and calibrate these variables as well as measuring the trigger and reconstruction efficiencies.

The invariant mass variable is validated through reconstruction of the J/ψ peak to begin with and eventually through the two-body $B_d \to K^+\pi^-$ decay. With the first $14\,\mathrm{nb}^{-1}$ of data we see a resolution of $16\,\mathrm{MeV}/c^2$ which is close to the anticipation from our simulations. Further improvements in this will happen with more data that allow for a detailed alignment.

The reconstruction efficiency is validated through a *tag-and-probe* method where one of the muons (the tag) in a J/ψ decay is fully identified in the muon system, while the other muon (the probe) is just identified through its tracks and the presence of a minimum ionising signal in the calorimeter. In this way one can infer the presence of a muon in the muon system and then check for the efficiency of actually finding it. In

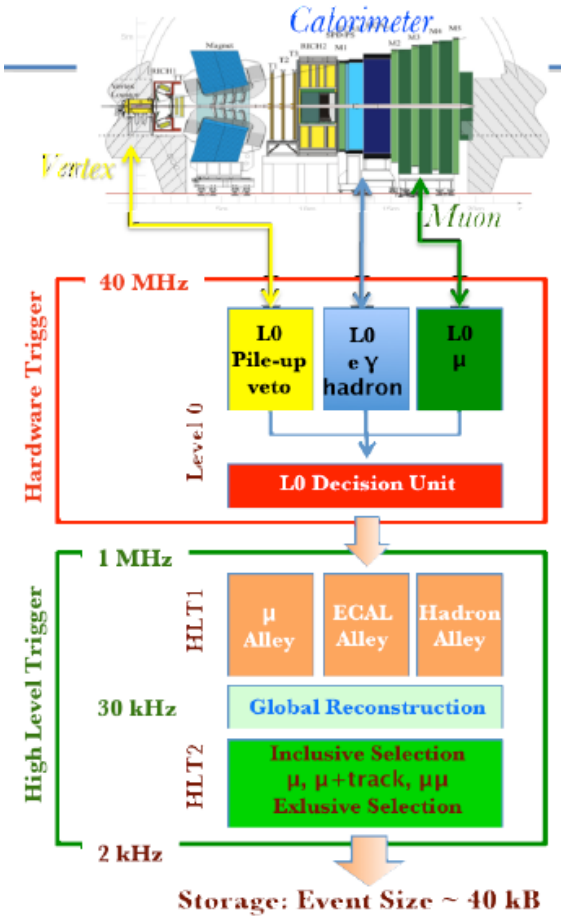

Figure 1. The LHCb trigger system. The first trigger is implemented in hardware and uses information from the calorimeters, the vertex detector and the muon system. The software trigger uses information from the full detector and performs eventually a full event reconstruction.

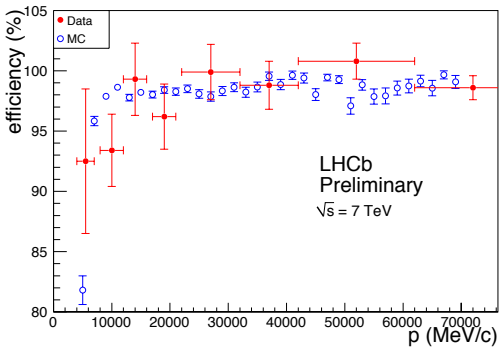

Figure 2. The efficiency of reconstructing muons as a function of momentum. The red (solid) points are the measurements on data, and the blue (open) points is the expectation from our simulation.

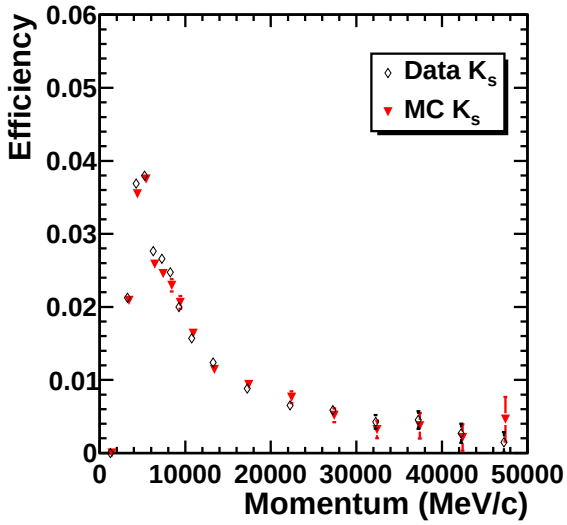

Figure 3. The efficiency of mis-identifying a pion from a K^0_S decay as a muon as a function of pion momentum. Data is the black diamonds and the expectations from simulation are red triangles.

Fig. 2 the efficiency as a function of momentum is compared between the data and our expectations from simulations. Within errors, the efficiencies are the same. Just as important for muon identification is to have a low mis-identification efficiency for pions. The mis-identification is dominated by decays in flight which can clearly be seen in Fig. 3 where the mis-identification efficiency rises at low momenta. In data this is measured through kinematic identification of pions coming from K^0_S decays.

The geometrical likelihood will for the final analysis be validated using two-body hadronic B decays which have identical kinematics to the signal. Until sufficient statistics are available for this, the individual contributions to the geometrical likelihood are evaluated on control channels. An example of this is the vertex χ^2 of the two muons from a J/ψ decay where the background subtracted distribution in the data compares well to the distribution from a simulated inclusive J/ψ sample.

The validation carried out so far gives us a high confidence in making projections for the future performance. In Fig. 4 we show the expected exclusion limit we can set at the 90% confidence limit as a function of integrated luminosity. It can be see that the data from 2011 should allow us to produce the worlds best limit or alternatively make a discovery.

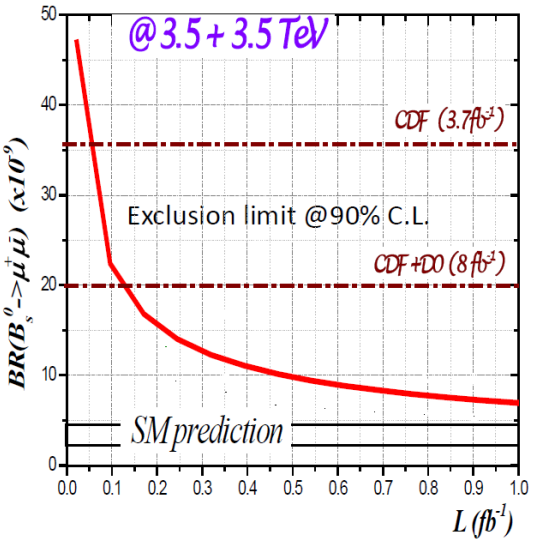

Figure 4. The expected exclusion limit for the $B_s \to \mu^+\mu^-$ decay as a function of integrated luminosity.

4. Radiative decays

The 1993 discovery of $B \to K^*\gamma$ [2] was the first observation of radiative penguin decays. It confirmed straight away that the SM was the dominant contributor to the decay. Since then, the main focus has been on measuring the inclusive $b \to s\gamma$ branching ratio, where the theoretical uncertainty is small. A direction that has only been exploited with limited precision so far, is the contribution of the right handed operator $\mathcal{C}_7^{'}$. As the left and right handed components do not interfere, the inclusive BR depends on $|\mathcal{C}_7|^2 + |\mathcal{C}_7^{'}|^2$ meaning that if $\mathcal{C}_7^{'}$ was even at the 20% level of $\mathcal{C}_7$, it would only add 4% to the inclusive BR, which is well below the theoretical uncertainty.

To explore a right handed component of the amplitude, it is required to explore methods where there is direct sensitivity to the left and right handed components. At first thought this would require the ability to measure the polarisation of the final state photon, which is not possible in a high energy physics experiment; however, the presence of B oscillations makes it possible anyway to get direct sensitivity. One such method is to look for the time dependent CP asymmetry in the CP eigenstate $B_d \to K^{*0}\gamma$, with $K^{*0} \to K^0_S\pi^0$. Such an analysis has been performed by *BABAR* [3] and BELLE [4,5] with a sensitivity at the 20% level for a right handed component. At LHCb, the measurement is best performed by looking at the time dependence of the decay $B_s \to \phi\gamma$, with $\phi \to K^+K^-$. As shown in [6], one can take advantage of the expected large value of $\Delta\Gamma$ in the B_s system to avoid the need for a flavour tagged analysis.

The performance in LHCb of the $B_s \to \phi\gamma$ depends most crucially on the performance of the calorimeter. The energy calibration of the

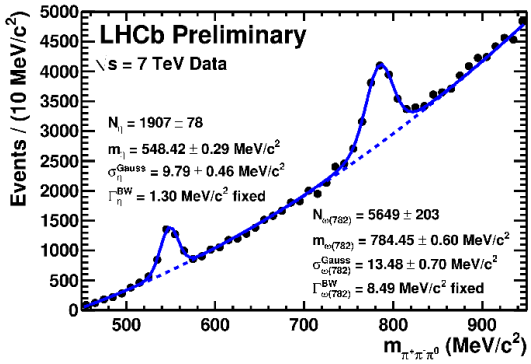

Figure 5. The reconstruction of the η and the ω in the first $3.4\,\mathrm{nb}^{-1}$ of data. The position of the peaks and their widths are in good agreement with the simulation of the detector.

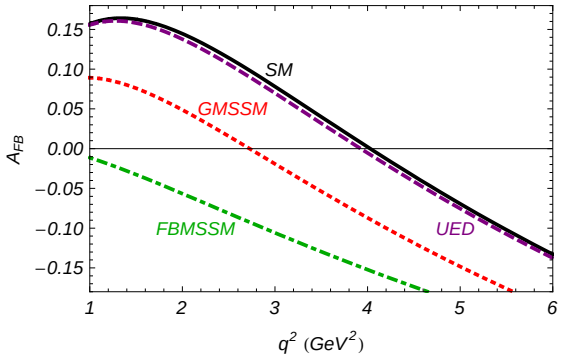

Figure 6. Predictions of the forward-backward asymmetry as a function of q^2 in a range of different new physics models.The dashed lines show a prediction from a universal extra dimensions (UED) model, a non-minimal flavour violating supersymmetric model (GMSSM) and a flavour blind supersymmetric model (FBMSSM). Details to be found in [8].

calorimeter has only just started. In Fig. 5 we show the peaks of the η and the ω to the $\pi^+\pi^-\pi^0$ final state. Both the central value of the peak and the width fit with expectations from simulations. The photons reconstructed from the π^0 decays are of a much lower energy than what will be the case for the photons from radiative B decays but is the best sample available. With higher statistics, the radiative $B_d \to K^{*0}\gamma$ decay will itself be used for for calibrating the calorimeter.

In a nominal LHCb year of $2\,\mathrm{fb}^{-1}$ the untagged measurement of $B_s \to \phi\gamma$ will give a resolution of around 10% for a right handed component.The signal is expected to have little background but the calibration of the lifetime measurement will be a challenge in order to keep the measurement statistics limited in the longer term.

5. $B_d \to K^{*0}\mu^+\mu^-$

The $B_d \to K^{*0}\mu^+\mu^-$ decay is a unique laboratory for the observation of NP. The two muons in the final state gives it a clear signature at a hadron collider, the theoretical predictions are precise and it has a sensitivity to left and right handed currents as well as the interference between $\mathcal{C}_7$ and the vector and axial vector couplings of $\mathcal{C}_9$ and $\mathcal{C}_{10}$. The sensitivity of the decay to NP is reviewed in many places; two recent examples are [7,8].

The most well known observable is the forward-backward asymmetry, A_{FB}, which is defined as the asymmetry of forward relative to backward going muons in the rest frame of the dimuon with respect to the B-meson direction of flight. When measured as a function of the invariant mass squared of the muon pair, q^2, the point where it cross zero has a small theoretical uncertainty and a high sensitivity to new physics. The sensi-

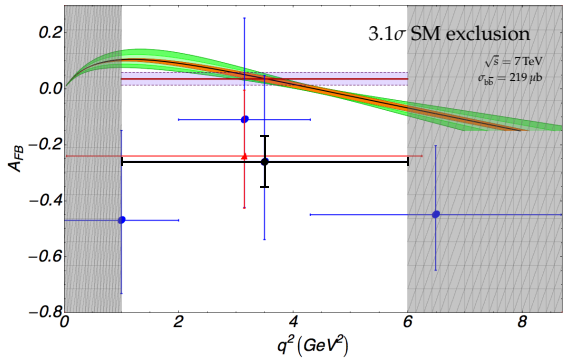

Figure 7. The measurements of $A_{\rm FB}$ from *BABAR* (red) and BELLE (blue). The expected experimental resolution of LHCb with $0.5\,{\rm fb}^{-1}$ is overlaid in black, with the assumption of the BELLEresult as the central value. It can be seen that this has the prospect of excluding the SM. The theoretical SM band and average value are taken from [7].

tivity to a range of different NP models is shown in Fig. 6 with the models from [8]. The current measurements from *BABAR* [9], BELLE [10] and CDF [11] all have limited statistics and are not yet able to say anything about the zero crossing point. Nevertheless the most accurate result from BELLE has a sign of $A_{\rm FB}$ in the region of low q^2 which is not the expected one from the SM.

In Fig. 7 previous measurements are illustrated together with a speculative measurement from LHCb with just $0.5\,{\rm fb}^{-1}$ of data and assuming the BELLE central value in the bin of $1\,{\rm GeV}^2 < q^2 < 6\,{\rm GeV}^2$ where the theoretical uncertainties are the smallest. It can be seen that the data taken during 2011 has the potential to show up a strong deviation from the SM in this channel. A precision measurement of the zero point in $A_{\rm FB}$ will be possible with a dataset of $2\,{\rm fb}^{-1}$.

6. Conclusion

The LHCb detector is fully functional and is collecting data from the proton-proton collisions at a centre-of-mass energy of 7 TeV. Through the use of control channels, we have shown that the detector performs well and is ready for providing exciting new results on rare decays with the data taken during 2010 for $B_s \to \mu^+\mu^-$ and for $B_s \to \phi\gamma$ and $B_d \to K^{*0}\mu^+\mu^-$ with data from 2011.

REFERENCES

1. Andrzej J. Buras. Flavour Theory: 2009. *PoS*, EPS-HEP2009:024, 2009.
2. R. Ammar et al. Evidence for penguins: First observation of $B \to K^*(892)\gamma$. *Phys. Rev. Lett.*, 71:674–678, 1993.
3. Bernard Aubert et al. Measurement of the time-dependent CP-violating asymmetry in $B^0 \to K^0_S\pi^0\gamma$ decays. *Phys. Rev.*, D72:051103, 2005.
4. Y. Ushiroda et al. Time-Dependent *CP* Asymmetries in $B^0t0K^0_S\pi^0\gamma$ transitions. *Phys.Rev.*, D74:111104, 2006.
5. J. Li et al. Time-dependent *CP* Asymmetries in $B^0 \to K^0_S\rho^0\gamma$ Decays. *Phys.Rev.Lett.*, 101:251601, 2008.
6. Franz Muheim, Yuehong Xie, and Roman Zwicky. Exploiting the width difference in $B_s \to \phi\gamma$. *Phys.Lett.*, B664:174–179, 2008.
7. U. Egede, T. Hurth, J. Matias, M. Ramon, and W. Reece. New observables in the decay mode $\overline{B}_d \to \overline{K}^{*0}\ell^+\ell^-$. *JHEP*, 11:032, 2008.
8. Wolfgang Altmannshofer et al. Symmetries and Asymmetries of $B \to K^*\mu^+\mu^-$ Decays in the Standard Model and Beyond. *JHEP*, 01:019, 2009.
9. Bernard Aubert et al. Measurements of branching fractions, rate asymmetries, and angular distributions in the rare decays $B \to K\ell^+\ell^-$ and $B \to K^*\ell^+\ell^-$. *Phys. Rev.*, D73:092001, 2006.
10. J. T. Wei et al. Measurement of the Differential Branching Fraction and Forward-Backward Asymmetry for $B \to K^{(*)}\ell^+\ell^-$. *Phys. Rev. Lett.*, 103:171801, 2009.
11. T. Aaltonen et al. Search for the Rare Decays $B^+ \to \mu^+\mu^-K^+$, $B^0 \to \mu^+\mu^-K^{*0}(892)$, and $B^0_s \to \mu^+\mu^-\phi$ at CDF. *Phys.Rev.*, D79:011104, 2009.